

The European heat wave of 2018 and its promotion of the ozone climate penalty in southwest Sweden

Julia M. Johansson¹, Ågot K. Watne², Per Erik Karlsson³,
Gunilla Pihl Karlsson³, Helena Danielsson³, Camilla Andersson⁴ and
Håkan Pleijel¹*

¹ University of Gothenburg, Biological and Environmental Sciences, P.O. Box 461, SE-40530 Göteborg, Sweden (*corresponding author's e-mail: hakan.pleijel@bioenv.gu.se)

² City of Gothenburg, Environment Administration, Box 7012, 402 31 Göteborg, Sweden

³ IVL Swedish Environmental Research Institute Inc., P.O. Box 53021, SE-40014 Göteborg, Sweden

⁴ Swedish Meteorological and Hydrological Institute, SE-60176 Norrköping, Sweden

Received 1 Nov. 2019, final version received 28 Feb. 2020, accepted 4 Mar. 2020

Johansson J.M., Watne Å.K., Karlsson P.E., Karlsson G.P., Danielsson H., Andersson C. & Pleijel H. 2020: The European heat wave of 2018 and its promotion of the ozone climate penalty in southwest Sweden. *Boreal Env. Res.* 25: 39–50.

The ozone concentration ($[O_3]$), temperature (T) and vapour pressure deficit (VPD) during the 2018 heat wave (HW) was compared with conditions from 2013–2017. The study included one coastal and two inland sites in southwest Sweden. The positive relationship between $[O_3]$ and T was stronger in 2018. The average daytime T from April–September was higher by 2.0–2.4°C in 2018. The VPD was strongly and positively affected by the 2018 HW. The daytime mean $[O_3]$ was enhanced by 7–12% in 2018. The relationship between hourly daytime $[O_3]$ and T , as well as that between the daily maximum $[O_3]$ and daily maximum T , was steeper in 2018. The stronger promotion of $[O_3]$ by T in 2018 was possibly partly a result of dry conditions causing stomatal closure of vegetation and thus a weaker O_3 sink. If HWs like that in 2018 become more common, they can be expected to promote higher $[O_3]$ and risk larger health and ecosystem effects.

Introduction

Tropospheric ozone (O_3) is a secondary, regional air pollutant formed in photochemical reactions from the precursors of nitrogen oxides (NO_x), volatile organic compounds (VOCs including CH_4) and carbon monoxide (CO). Ozone has significant effects on human health (Nuvolone *et al.* 2018) and vegetation (Mills *et al.* 2018) and is a greenhouse gas of large importance (Monks *et al.* 2015). High concentrations of ozone, $[O_3]$, are enhanced by anticyclonic weather conditions with warm and sunny weather, promoting photochemi-

cal activity (Tang *et al.* 2009, Bloomer *et al.* 2009, Zhang *et al.* 2017). In line with this, wide areas of Europe experienced an extended period of strongly elevated $[O_3]$ during a pronounced heat wave (HW) in 2003 (e.g., Pellegrini *et al.* 2007, Solberg *et al.* 2008).

It has been estimated, using epidemiological techniques, that during the 2003 European HW, which culminated during two weeks in August, both high temperatures (T) and elevated $[O_3]$ contributed to excess mortality, for example in France (Filleul *et al.* 2006, Fischer *et al.* 2004, Stedman 2004, Dear *et al.* 2005). The study by Dear *et*

al. (2005), examining the effects of temperature and ozone on mortality in twelve French cities during that HW, found that in Paris the elevated $[O_3]$ accounted for about half of the increased daily mortality. This demonstrates how episodes of enhanced temperature, e.g., as a result of climate change, severely can affect the air quality and consequently the impacts on human health by promoting formation of tropospheric O_3 , in addition to the temperature effect on human health as such (Doherty *et al.* 2017, Nolte *et al.* 2018).

HWs are expected to increase in frequency and intensity in the future due to climate change (e.g., Russo *et al.* 2014). Consequently, periods with strongly elevated $[O_3]$ can be expected to become more frequent (Kalisa *et al.* 2018), provided that emissions of O_3 precursors are not significantly reduced. The summer of 2018 was for large parts of Europe an unusually warm and dry period, which resulted in numerous record-breaking temperatures and drought events that affected especially northern and central Europe, including Scandinavia (World Meteorological Organization 2019).

Sweden was one of the countries significantly affected by the 2018 HW, experiencing wildfires, reduced crop-yields, low groundwater and surface water levels as well as increased human health risks for sensitive groups (Sjökvist *et al.* 2019, World Meteorological Organization 2019). Measurements at official national weather stations showed that the whole summer was, on average, 2–4 °C above normal for south Sweden. For most stations, it was the warmest summer ever registered, with temperatures representing typical summers in year 2100 under the pessimistic RCP8.5 scenario along the Baltic coast and between the RCP4.5 and RCP8.5 scenarios in the rest of the country (Sjökvist *et al.* 2019). In addition, the spring and summer of 2018 had less precipitation and more sunshine hours than usual for a large part of the country (Sjökvist *et al.* 2019).

Several factors contribute to the enhanced $[O_3]$ during HWs. These include high levels of solar radiation, stimulation of O_3 precursor emissions such as isoprene and other biogenic VOC from vegetation (Abeleira and Farmer 2017) and release of other VOCs and NO_x from wildfires (Brey and Fischer 2016). Furthermore, high T promotes photochemical activity as well as

reduced destruction of O_3 at the Earth surface (Solberg *et al.* 2008). A large fraction of the O_3 deposition at the Earth surface takes place by plant stomatal uptake (Emberson *et al.* 2013). This process accounts, on average, for 40–60% of the terrestrial ecosystem O_3 uptake (Cieslik 2004, Fowler *et al.* 2001). During extended periods of drought and heat, vegetation is likely to absorb less O_3 than otherwise, since plants close their stomata under these conditions to avoid desiccation (Buckley 2019). A lower stomatal uptake of O_3 leads to a rise in $[O_3]$ at ground level as suggested by observations (Pio *et al.* 2000) and modelling (Vieno *et al.* 2010). Similarly, Andersson and Engardt (2010) found in a modelling study that a large part of the promoted ground-level $[O_3]$ under climate change in Europe was due to reduced dry deposition. Thus, a reduced surface O_3 sink will promote high ground-level $[O_3]$ during extended HWs beyond the effect of weather enhanced photochemical O_3 production in sunny and calm conditions (Varotsos *et al.* 2019).

From a plant physiological perspective, drought can be induced by both dry soil (lack of available water) and dry air (representing a strong sink for water vapour from plant transpiration). The drying power of the air can be quantified by the water vapour pressure deficit (VPD). The VPD is the difference between potential and actual vapour pressure at prevailing T (Campbell and Norman 1998). A high VPD is known to strongly promote stomatal closure in plants, thus reducing O_3 uptake (Buckley 2019).

As shown in the modelling study by Emberson *et al.* (2013), a climate change scenario with stronger, prolonged HWs may lead to dangerously elevated $[O_3]$ during extended periods of time. This was further supported by a global modelling study by Meehl *et al.* (2018). These authors also emphasized the importance of O_3 precursors for this effect.

Bloomer *et al.* (2009) used the phrase, “climate penalty” to denote the additional $[O_3]$ obtained for a certain increase in T . They showed strong evidence of such an ozone climate penalty for a wide range of sites in four regions of USA, with respect to average concentrations as well as for different percentiles of $[O_3]$. The degree of $[O_3]$ dependence on T was highly consistent and indicated to be sensitive to the level of NO_x emis-

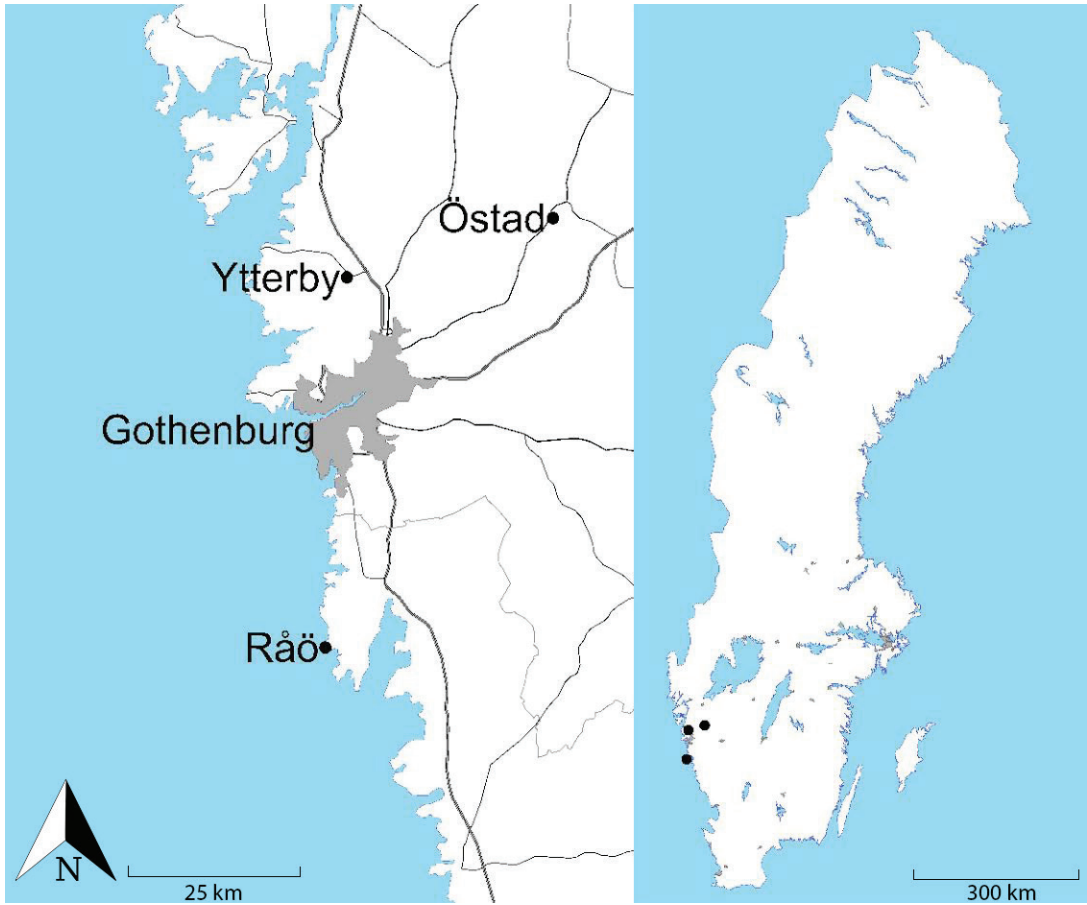


Fig. 1. Map showing the location of the three O_3 monitoring sites Råö (57.39383°N, 11.9140°E), Ytterby (57.8635°N, 11.9215°E) and Östad (57.9525°N, 12.4035°E) in relation to the city of Gothenburg and the Swedish west coast.

sions. The O_3 climate penalty from rising T has also been studied by Varotsos *et al.* (2019) and Peters *et al.* (2018) with results similar to those of Bloomer *et al.* (2009). Furthermore, Otero *et al.* (2018), in a large model inter-comparison of meteorological drivers of surface O_3 over Europe, investigated the $[O_3]$ – T relationship in different parts of Europe and compared with observations from monitoring stations. These authors found that, to a large extent, current models reproduce the observed climate penalty relatively well.

Partly linked to the diurnal solar cycle, both $[O_3]$ and T have typical diurnal cycles, which are at least partly statistically correlated. The strength of the $[O_3]$ and T diurnal cycles depends on local climate, being e.g., stronger at inland vs. coastal locations (Klingberg *et al.* 2012). Consequently, to investigate the details of the ozone climate

penalty, it is motivated to analyse the relationship between $[O_3]$ and T specifically during the mid-day hours for which the diurnal cycles of $[O_3]$ and T are of limited importance. In this way, the analysis of the relationship between $[O_3]$ and T becomes essentially independent of (auto)correlated diurnal cycles.

The temperatures of 2018 were elevated for an extended period of time for northern and western Europe, persisting through late spring and summer (WMO, 2019). During this time, high $[O_3]$ were observed over wide areas of Europe, including south Sweden (<http://www.smhi.se>) and Norway (<http://www.nilu.no>). In order to investigate the association between $[O_3]$ and the HW in 2018, we analysed data from three sites in SW Sweden for the 2013–2018 growing season (April–September).

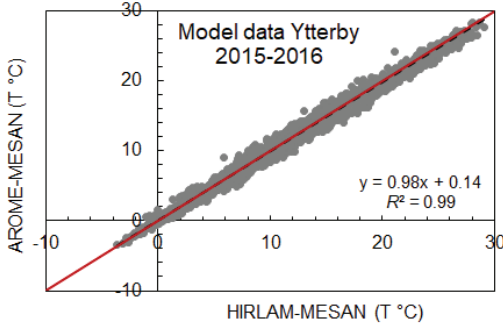


Fig 2. Temperature data extracted from two meteorological data models, Arome-Mesan and Hirlam-Mesan, plotted against each other for the Ytterby site and the two years (2015–2016) for which overlapping data were available. The dotted black trend line represents the relationship for plotted data while the solid red trend line shows the theoretical 1:1 relationship as a comparison.

In the present paper, we investigate the ozone climate penalty suggested by Bloomer *et al.* (2009) for south Sweden. We further investigate if the climate penalty is stronger in a HW situation, i.e., that the slope coefficient of the relationship between $[O_3]$ and T is larger under the dry HW conditions, as can be expected under warm and dry conditions. The following research questions were addressed:

- To what extent was the growing season of 2018 different from 2013–2017 with respect to $[O_3]$, T and VPD in southwest Sweden?
- Was there an association between $[O_3]$ and T in line with the ozone climate penalty suggested by Bloomer *et al.* (2009)?
- If yes, was the sensitivity of $[O_3]$ to T larger in 2018 as compared with 2013–2017, as could be hypothesized to result from the drought-induced reduced land-surface sink of O_3 under HW extended drought and high VPD?
- Was there a difference in the HW effect on $[O_3]$ between the coastal and inland sites?

Material and methods

Data

This study used hourly ozone data from three different monitoring stations in southwest

Sweden (Fig. 1). Råö is a coastal, rural site (57.39383° N, 11.9140° E). The O_3 monitoring point is situated 20 meters from the shore-line, 5 m a.s.l. Ytterby is a suburban, inland site located 12 m a.s.l. near the small town of Kungälv (57.8635° N, 11.9215° E). Östad is a rural, inland site (57.9525° N, 12.4035° E). Here, O_3 monitoring is made at an open field, 65 m a.s.l. The locations for Ytterby and Östad sites are situated topographically low compared with surrounding terrain. Ozone monitors (Thermo Scientific 49c at Östad, Thermo Scientific 49i at Råö and Ytterby) were regularly calibrated.

Hourly temperature data for Ytterby and relative humidity for all three sites were extracted from the MESAN datasets. These are based on a sophisticated combination of observed temperatures and humidities at the 2 m height and modelled fields by the numerical weather prediction models HIRLAM (11 km resolution; HIRLAM-MESAN) for 2013–2016 and AROME (0.025 degrees resolution; AROME-MESAN) for 2016–2018 (Häggmark *et al.* 2000, Bengtsson *et al.* 2017). The modelled data used in this study is therefore a combination of the two data sets. Overlapping data from the two sets were plotted against each other to compare how the difference in resolution and method influenced the different values. The data from the two sets were strongly correlated with a very small bias (Fig. 2). We also compared modelled and measured temperature data for Östad and Råö (data not shown). For Östad the agreement between modelled and measured data was good ($y = 1.03x - 0.57$; $R^2 = 0.889$), whereas the disagreement was somewhat larger for Råö ($y = 1.23x - 1.91$; $R^2 = 0.897$).

At Östad and Råö, hourly temperatures were measured using a Tinytags (INTAB Interface-Teknik AB, Stenkullen, Sweden) TGP-4500 sensors/loggers enclosed in radiation shields with a reflective cover. The Tinytag at Östad was calibrated against a continuously measuring temperature probe (Rotronic Hygroclip (2013–2015), Rotronic HC2-S3 (2016–2018)) located at Östad. The Tinytag at Råö was calibrated against the Östad Tinytag.

The data used in this study are hourly observations from 2013–2018, for the growing season,

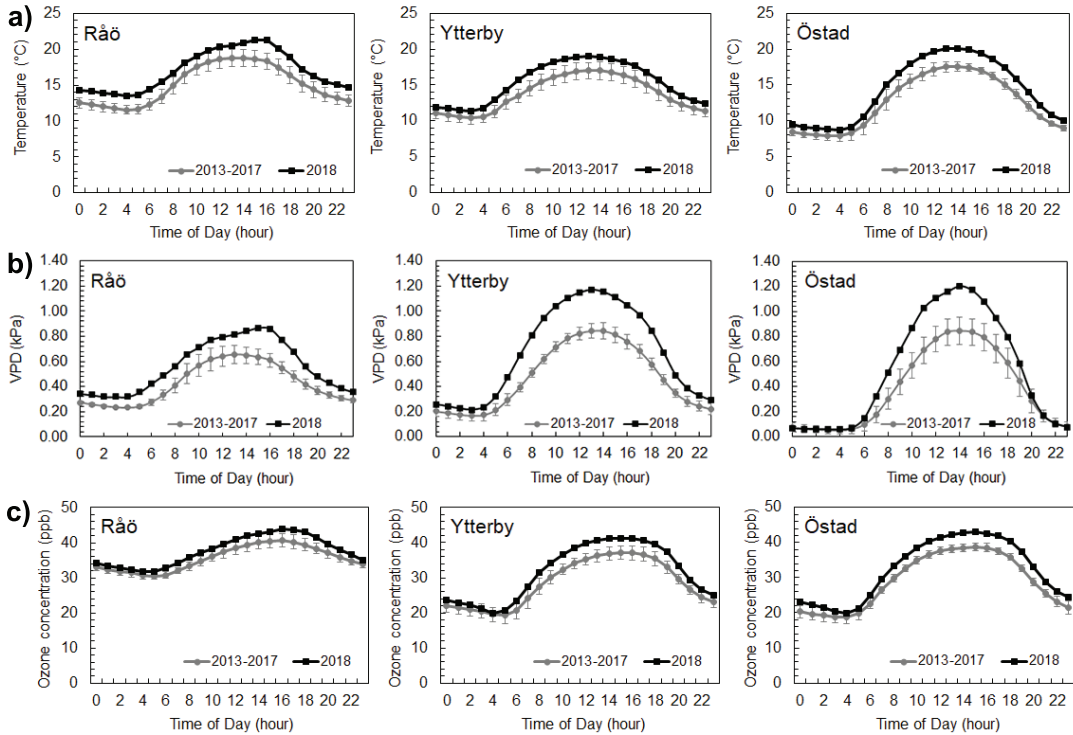


Fig. 3. Average diurnal profiles (Apr.–Sep.) of (a) air temperature, (b) water vapour pressure deficit (VPD) and (c) ozone concentration $[O_3]$, at Råö, Ytterby and Östad for 2018 and 2013–2017. The error bars for 2013–2017 represent one standard deviation for the five different years.

from 1 April to 30 September. The daytime and night-time hours were defined as 08:00–20:00 and 20:00–08:00, respectively. Analysis of relationships between $[O_3]$ and T was also made for the daily time window (10:00–16:00) as well as for daily maxima $[O_3]$ and T .

The water vapour pressure deficit (VPD) was calculated as the difference in water vapour pressure between saturated and ambient air at prevailing air temperature. It was calculated from relative humidity and T according to Campbell and Norman (1998).

Estimation of the O_3 climate penalty from temperature

Firstly, we evaluated the concept of climate penalty, i.e., $[O_3]$ positively depending on temperature, as defined by Bloomer *et al.* (2009), by plotting the average and the 95th-, 75th-, 50th-, 25th-, and 5th-percentiles of distributions

of hourly $[O_3]$ vs T for 3°C temperature bins in the interval 15–29°C, for daytime data and 4–18°C for night-time data. The O_3 climate penalty was also estimated as the linear slope coefficients (rate of increase in $[O_3]$ with the increase in T) from regression-based scatterplots using all daytime hourly $[O_3]$ and T data (i.e., not using temperature bins). Finally, the relationship between daily maximum $[O_3]$ and daily maximum T was analysed. For all cases, the relationship between $[O_3]$ and T of 2018 was compared with 2013–2017.

Statistical analyses

Linear regression was used to assess the significance of the relationships between hourly $[O_3]$ and T as well as between daily maximum $[O_3]$ and daily maximum T . To test if the regression slope coefficients for relationships between O_3 and T were significantly different between

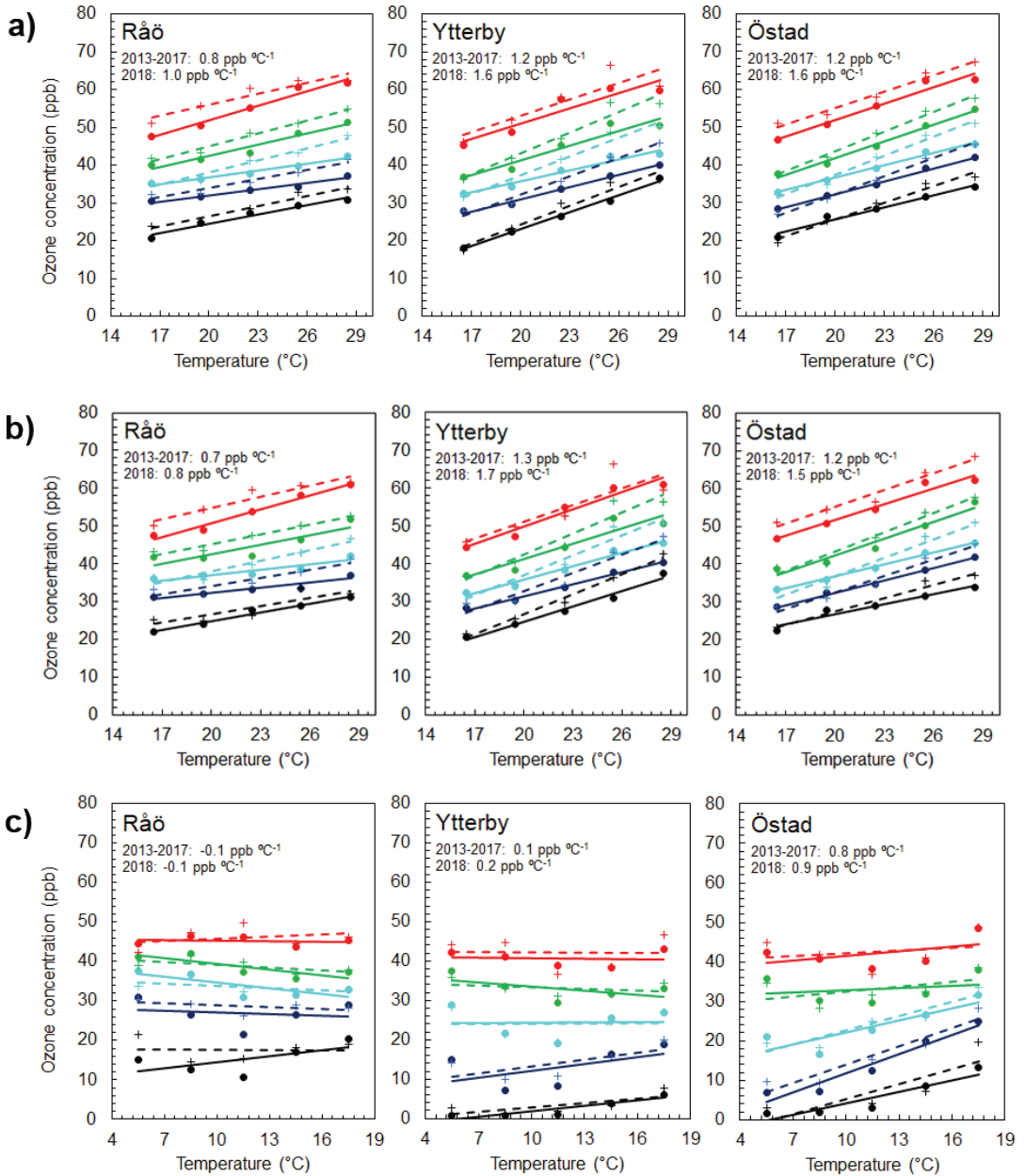


Fig. 4. Ozone concentrations (Apr.–Sep.), from (a) 08:00–20:00, (b) 10:00–16:00 and (c) 20:00–08:00. The 5th- (black), 25th- (blue), 50th- (cyan), 75th- (green) and 95th-percentiles (red) at different 3°C bins in relation to temperature for 2013–2017 (solid line) and 2018 (dotted line) at Råö, Ytterby and Östad, are shown. Below the name of the site, the average rate of increase of $[O_3]$ with T based on the 3°C bins is given.

2013–2017 and 2018, a regression analysis was performed with a so-called interaction term included in the regression model. The statistics was done in the software SPSS ver. 22 (IBM).

Results

Average diurnal variation in $[O_3]$, T and VPD in 2018 compared with 2013–2017

At all three sites, $[O_3]$, T and VPD were, on average, considerably higher in 2018 than in 2013–2017, both during daytime and night-time (Fig. 3, Table 1).

In general, differences between 2018 and 2013–2017 were larger during the day than during the night. The diurnal variation was the smallest for Råö and the largest for Östad for all the variables, reflecting the contrast between coastal and inland climates. Ytterby showed a pattern similar to Östad, but with somewhat smaller diurnal variations, likely reflecting a position closer to the coast. The most striking difference between 2018 and 2013–2017 was for VPD. Daytime VPD was increased by 43% at Ytterby, 42% at Östad and 32% at Råö (Table 1). Temperature was higher by $\geq 2^\circ\text{C}$ in the growing season of 2018 at all sites as a growing season average, while $[O_3]$ was enhanced in 2018 in

relation to 2013–2017 by 7%, 12% and 11% at Råö, Ytterby and Östad, respectively.

Relationships between $[O_3]$ and T in 2018 vs 2013–2017 during daytime, mid-day and night-time on average and for different $[O_3]$ percentiles

In Fig. 4a, following Bloomer *et al.* (2009), the relationship of $[O_3]$ in 3°C bins in relation to temperature is presented for different percentiles of $[O_3]$. In all cases, the relationship is clear and essentially linear. Except at the 95th percentile, the relationships were steeper in 2018 than 2013–2017. The increase in $[O_3]$ with T was somewhat weaker for coastal Råö ($1.0 \text{ ppb } ^\circ\text{C}^{-1}$) compared to inland Ytterby and Östad ($1.6 \text{ ppb } ^\circ\text{C}^{-1}$ for both sites).

In Fig. 4b, the corresponding relationships for the shorter time window (10:00–16:00) are presented to minimize the influence of the diurnal variation in $[O_3]$ and T . However, the relationships changed very little by reducing the daily time window evaluated from 08:00–20:00 to 10:00–16:00, indicating that the analysis was not sensitive to the used time windows.

In night-time conditions (Fig. 4c), the pattern was very different. For the higher percentiles, there was essentially no relationship between

Table 1. Daytime (08:00–20:00) average temperature, VPD (water vapour pressure deficit) and ozone concentration for the growing season (1 April–30 September) at Råö, Ytterby and Östad. Also, the difference between the two observation periods are given as absolute and relative values.

	2013–2017	2018	Difference	Percent
Temperature ($^\circ\text{C}$)				
Råö	17.5	19.5	2.0	n.a.
Ytterby	15.7	17.9	2.2	n.a.
Östad	15.9	18.3	2.4	n.a.
VPD (kPa)				
Råö	0.56	0.74	0.18	32%
Ytterby	0.70	1.00	0.30	43%
Östad	0.65	0.93	0.28	42%
Ozone (ppb)				
Råö	38.3	40.9	2.68	7%
Ytterby	34.4	38.6	4.22	12%
Östad	36.0	40.0	4.03	11%

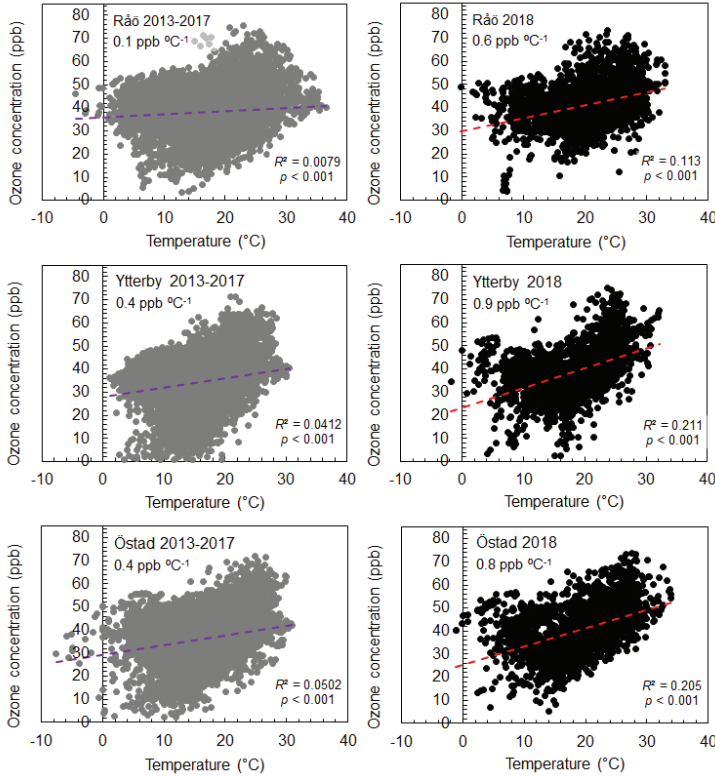


Fig. 5. Relationship between hourly daytime (08:00–20:00) ozone concentration and temperature (Apr.–Sep.) at Råö, Ytterby and Östad for 2013–2017 (lilac regression line) and 2018 (red regression line).

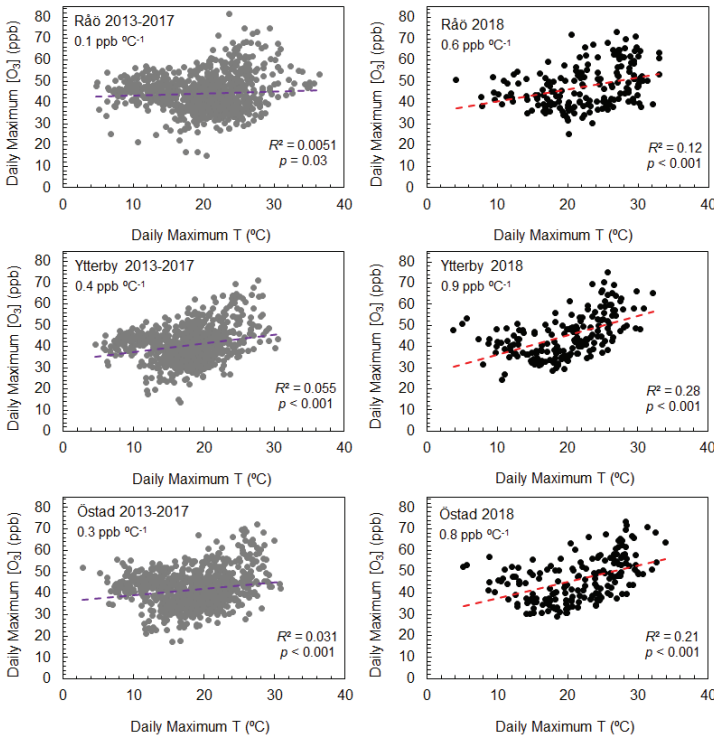


Fig. 6. Relationship between maximum hourly daytime (08:00–20:00) ozone concentration and maximum hourly temperature (Apr.–Sep.) at Råö, Ytterby and Östad for 2013–2017 (lilac regression line) and 2018 (red regression line).

$[O_3]$ and T . At Råö, no clear relationships were observed also for the lower percentiles, while for Ytterby, and even more for Östad, positive $[O_3]$ – T relations were observed for lower percentiles. The night-time relationships in 2018 were similar to those in 2013–2017.

Relationships between daytime and daily maximum hourly $[O_3]$ and T

Figure 5 displays the relationships between all daytime hourly $[O_3]$ and hourly T in 2013–2017 and 2018 for Råö, Ytterby and Östad. For all the three sites, the slope coefficient was larger in 2018 than in 2013–2017. In all the cases, the difference between the two periods was statistically significant ($p < 0.001$). At the coastal site Råö the slope coefficients (unit: ppb °C⁻¹) (2018: 0.6; 2013–2017: 0.1) were smaller than those at Ytterby (2018: 0.9; 2013–2017: 0.4) and Östad (2018: 0.8; 2013–2017: 0.4), the latter two locations differing relatively little from each other. The contrast between 2018 and 2013–2017 was the strongest for Råö.

In Fig. 6, the relationships between hourly daily maximum $[O_3]$ and hourly daily maximum T are compared between 2013–2017 and 2018 for Råö (slope coefficient 2018: 0.6; 2013–2017: 0.1), Ytterby (2018: 0.9; 2013–2017: 0.4) and Östad (2018: 0.8; 2013–2017: 0.3). The difference between the slope coefficients for 2018 and 2013–2017 was strongly statistically significant for all three sites ($p < 0.001$). The general pattern is similar to that of Fig. 5. Intercepts are higher in Fig. 6, but the slopes and R^2 values did not differ much from Fig. 5. It can be noted that in both Fig. 5 and Fig. 6, the R^2 values were considerably higher in 2018 compared with 2013–2017.

Discussion

The most important result of our study is that the relationship between $[O_3]$ and T , observed in several earlier studies (e.g., Bloomer *et al.* 2009, Petres *et al.* 2018, Varotsos *et al.* 2019), was steeper in the heat wave growing season of 2018 compared with 2013–2017. This sug-

gests that under extended HW conditions, the enhancement of $[O_3]$ by T is increased, which will increase the risk for human health effects from elevated $[O_3]$ — adding to the hazards from high T as such. A similar result was obtained by Varotsos *et al.* (2019) when analysing $[O_3]$ – T relationships during the 2003 and 2014 HWs in Europe, by analysing observations from a range of O_3 monitoring stations in Europe. Since the magnitude of extreme HWs are likely to become more common in a warming world (Russo *et al.* 2014), the associated promotion of high $[O_3]$ should be considered in assessments of human health and ecosystem implications of global warming in general and in association with HWs in particular.

We also investigated the relationship between $[O_3]$ and VPD using the same approach as for T (data not shown). There is indeed a positive relationship between $[O_3]$ and VPD, but not a steeper relationship in 2018 compared with 2013–2017, as for T .

The mechanisms of the HW promotion of $[O_3]$ enhancement need further investigation. However, the very dry conditions during the HW summer of 2018, evidenced by the large growing season elevation of VPD and the extremely low precipitation levels reported from official national weather stations (Sjövist *et al.* 2019), suggest that a reduced stomatal deposition, although not measured in our study, may be of significant importance for the additional $[O_3]$ promotion by T in 2018 compared with 2013–2017. This is in line with modelling results, such as those by Emberson *et al.* (2013), who investigated the substantial limiting effect of drought on the vegetation O_3 sink on surface level $[O_3]$ for simulated HW conditions in the United Kingdom. A significant role for reduced dry deposition under HW conditions is also supported by the modelling analysis of the 2003 HW and its causes (Vieno *et al.* 2003) and by the observation of the strong seasonality of O_3 deposition linked to the strong variation in humidity in Portugal (Pio *et al.* 2000). Obviously, there are also other factors that can contribute to the T dependence of $[O_3]$. These include T promotion of photochemistry as well as the associated high levels of solar radiation, stimulation of O_3 precursor emissions from vegetation (isoprene

and other biogenic VOC; Abeleira and Farmer 2017) and release of other VOCs and NO_x from wildfires (Brey and Fischer 2016). In addition, transport of warm air masses containing O_3 and its precursors from the south may occur in association with HWs in Scandinavia. However, what we need to understand about the pattern observed in this study is the stronger promotion of $[\text{O}_3]$ by T under extended HW conditions. For this, drought-induced stomatal closure and the following reduction in O_3 deposition seems to be a relevant candidate.

The comparison of the two different daily T windows, 08:00–20:00 and 10:00–16:00, did not reveal any substantial difference in the $[\text{O}_3]$ – T relationships based on $[\text{O}_3]$ for different T bins (Fig. 4a and b). This suggests that analysis for daytime conditions is not very sensitive to the time window used, although the larger amount of data available using the larger time window is an advantage. Correspondingly, when analysing hourly daytime data (Fig. 5) and daily maximum data (Fig. 6), the relationships between $[\text{O}_3]$ and T were very similar with respect to the slope coefficients, suggesting that the rise in $[\text{O}_3]$ with T in daytime conditions is rather general. In fact, the increase in the slope coefficient by the 2018 growing season compared with 2013–2017, being highly significant in all the cases, varied modestly from 0.38 to 0.51 among the six cases presented in Figs. 5 and 6.

A large difference was obtained for the rate of increase in $[\text{O}_3]$ with T when comparing the T bin analysis based on the approach introduced by Bloomer *et al.* (2009; see Fig. 4a and b) and the analysis based on all daytime hourly data (Figs. 5 and 6). The $[\text{O}_3]$ promotion by T was indicated to be substantially higher using the T bin approach. For example, for Östad in 2018, 1.6 ppb $^\circ\text{C}^{-1}$ was obtained with the T bin method while the method using hourly data resulted in a corresponding value of 0.8 ppb $^\circ\text{C}^{-1}$. The T bin approach offers the attractive opportunity to calculate percentiles, which reflect the distribution of $[\text{O}_3]$, but inevitably, the different T bins will contain a highly varying number of observations — the ones close to average temperatures many more than the T bins at the upper and lower ends of T . This allows for a bias from the proportionally stronger influence of the highest

and lowest T situations using the T bin approach, which potentially explains the difference from the method based on all data, where the large number of data points close to the average temperatures has a much larger influence on the result. An analysis based on hourly data, unlike that for binned data, satisfies the assumptions for regression analysis. Therefore, it offers statistical analysis of the difference in the slopes between the two observation periods.

In the study of Bloomer *et al.* (2009), the climate penalty based on the temperature bin approach for the more recent period investigated was on average 2.2 ppb $^\circ\text{C}^{-1}$ for the large region (eastern United States), whilst only 1.4 ppb $^\circ\text{C}^{-1}$ in the least O_3 -polluted region. The latter value is very similar to the average for the three sites included in our study, which was also 1.4 ppb $^\circ\text{C}^{-1}$.

Night-time data (Fig. 4c) showed a very different pattern from daytime (Fig. 4a). No enhancement of any T effect on $[\text{O}_3]$ by the 2018 HW conditions could be discerned. During the night, stomata are more or less closed. Thus, a HW effect based on altered stomatal O_3 deposition cannot be expected. For night-time conditions, the coastal site differed strongly from the inland sites, especially Östad, with respect to the $[\text{O}_3]$ – T relationships. The increase in night-time $[\text{O}_3]$ with T at the lower percentiles of $[\text{O}_3]$ at Östad and Ytterby can probably be explained by the influence of night-time stable stratification of the nocturnal boundary layer being much more frequent in inland sites compared with coastal sites (Pleijel *et al.* 2013). As shown by Klingberg *et al.* (2012), under these conditions, $[\text{O}_3]$ near the ground declines strongly because O_3 lost by deposition is not replenished by O_3 -richer air aloft (Garland and Derwent 1979). This effect will tend to be associated with lower T since the stable nocturnal boundary layer is a consequence of surface radiative cooling. Higher night-time $[\text{O}_3]$ (higher percentiles) are less likely to be associated with a very stable atmospheric stratification near the ground. In the night, no promotion of $[\text{O}_3]$ by T stimulating photochemistry can be expected in the absence of solar radiation to drive photochemical reactions. In effect, the $[\text{O}_3]$ – T relationship disappears for high percentiles at the inland sites and essentially for all

percentiles at the coastal site. The much lower likelihood of strong nocturnal inversions in the coastal environment (Klingberg *et al.* 2012) explains the general absence of a relationship between night-time $[O_3]$ and T , as well as the smaller diurnal variation in T , VPD and $[O_3]$, at the coastal site.

An important conclusion from the night-time results is that any analysis of the O_3 climate penalty from rising T should avoid the inclusion of night-time data. Firstly, the O_3 dynamics is, to large extent, unrelated to T during the night, at least at higher percentiles, i.e., there is no photochemistry which can be influenced by T . Secondly, night-time $[O_3]$ is highly sensitive to geographical location (Klingberg *et al.* 2012), which leads to the introduction of variation not related to the ozone climate penalty. Finally, the positive relationship between $[O_3]$ and T that may exist during the night in locations prone to nocturnal inversion is related to restricted vertical transport of O_3 .

Our investigation clearly shows that the growing season during the 2018 heat wave differed strongly and significantly from the preceding 5-year period with respect to $[O_3]$, T and VPD at the three investigated sites in SW Sweden. The ozone climate penalty was significantly larger during the 2018 HW compared with 2013–2017, highlighting the importance of extended, dry HWs for elevated $[O_3]$. The mechanisms behind this O_3 -promoting HW effect should be investigated in modelling and by observations, including the potentially large role of lower O_3 deposition in dry conditions. Finally, as pointed out by Emberson *et al.* (2013), the risk for climate-induced O_3 effects on human health have to be considered in analyses of the consequences of climate change.

Acknowledgements: This study was supported by the SCAC2 research programme funded by the Swedish Environmental Protection Agency. This research was also partly funded through the 2017–2018 Belmont Forum and BiodivERsA joint call for research proposals, under the BiodivScen ERA-Net COFUND programme, and with the funding organisations FORMAS, BMBF, ANR, AEI and AKA through the project BioDiv-Support (FORMAS Dnr 2018-02434). Finally, the project was supported by the Strategic Research Area MERGE (Modelling the Regional and Global Earth System, <https://www.merge.lu.se/>).

References

- Abeleira A.J. & Farmer D. 2017. Summer ozone in the northern Front Range metropolitan area: weekend-weekday effects, temperature dependencies, and the impact of drought. *Atmos. Chem. Phys.* 17: 6517–6529.
- Andersson C. & Engardt M. 2010. European ozone in a future climate: importance of changes in dry deposition and isoprene emissions. *J. Geophys. Res.* 115, D02303.
- Bloomer B.J., Stehr J.W., Piety C.A., Salawitch R.J. & Dickerson R.R. 2009. Observed relationships of ozone air pollution with temperature and emissions. *Geophys. Res. Lett.* 36: L09803.
- Bengtsson L., Andrae U., Aspelien T., Batrak Y., Calvo J., de Rooy W., Gleeson E., Hansen-Sass B., Homleid M., Hortal M., Ivarsson K.-I., Lenderink G., Niemelä S., Nielsen K. P., Onvlee J., Rontu L., Samuelsson P., Munoz D. S., Subias A., Tjmm S., Toll V., Yang X. & K oltzow M. . 2017. The HARMONIE-AROME model configuration in the ALADIN-HIRLAM NWP system. *Monthly Weather Review* 145: 1919–1935.
- Brey S.J. & Fischer E.V. 2016. Smoke in the city: how often and where does smoke impact summertime ozone in the United States? *Environ. Sci. Technol.* 50: 1288–1294.
- Buckley T.N. 2019 How do stomata respond to water status? *New Phytol.* 24: 21–36.
- Campbell G.S. & Norman J.M. 1998. *An Introduction to Environmental Biophysics*. 2nd ed. Springer-Verlag, New York-Berlin-Heidelberg.
- Cieslik S.A. 2004. Ozone uptake by various surface types: a comparison between dose and exposure. *Atmos. Environ.* 38: 2409–2420.
- Dear K., Ranmuthugala G., Kjellstr om T., Skinner C. & Hanigan I. 2005. Effects of temperature and ozone on daily mortality during the August 2003 heat wave in France. *Archives of Environmental and Occupational Health.* 60: 205–212.
- Doherty R.M., Heal M.R. & O’Connor F.M. 2017. Climate change impacts on human health over Europe through its effect on air quality. *Environ. Health* 16 (Suppl 1), 118, DOI 10.1186/s12940-017-0325-2.
- Emberson L.D., Kitwiroon N., Beevers S., B uker P. & Cinderby S. 2013. Scorched Earth: how will changes in the strength of the vegetation sink to ozone deposition affect human health and ecosystems? *Atmos. Chem. Phys.* 13: 6741–6755.
- Filleul L., Cassadou S., M edina S., Fabres P., Lefranc A., Eilstein D., Le Tertre A., Pascal L., Chardon B., Blanchard M., Declercq C., Jusot J.-F., Prouvost H. & Ledrans M. 2006. The relation between temperature, ozone, and mortality in nine French cities during the heat wave of 2003. *Environ. Health Persp.* 114: 1344–1347.
- Fischer P.H., Brunekreef B. & Lebreton E. 2004. Air pollution related deaths during the 2003 heat wave in the Netherlands. *Atmos. Environ.* 38: 1083–1085.
- Fowler D., Flechard C., Cape J.N., Storeton-West R. & Coyle M. 2001. Measurements of ozone deposition to vegetation quantifying the flux, the stomatal and non-stomatal components, *Water Air Soil Pollut.* 130: 63–74.

- Garland J.A. & Derwent R.G. 1979. Destruction at the ground and the diurnal cycle of concentration of ozone and other gases. *Q. J. Roy. Met. Soc.* 105: 169–183.
- Hägghmark L., Ivarsson K.I., Gollvik S., & Olofsson P.O. 2000. Mesan, an operational mesoscale analysis system. *Tellus* 52A: 2–20.
- Kalisa E., Fadlallah S., Amani M., Nahayo L. & Habiyaemye F. 2018. Temperature and air pollution relationship during heatwaves in Birmingham, UK. *Sustainable Cities and Society* 43: 111–120.
- Klingberg J., Karlsson P.E., Pihl Karlsson G., Hu Y., Chen D., Pleijel H. 2012. Variation in ozone exposure in the landscape of southern Sweden with consideration of topography and coastal climate. *Atmos. Environ.* 47: 252–260.
- Meehl G.A., Tebaldi C., Tilmes S., Lamarque J.-F., Bates S., Pendergrass A & Lombardozzi D. 2018. Future heat waves and surface ozone. *Environ. Res. Lett.* 13: 064004.
- Mills G., Sharps K., Simpson D., Pleijel H., Broberg M., Uddling J., Jaramillo F., Davies W.J., Dentener F., Van den Berg M., Agrawal M., Agrawal S.B., Ainsworth E.A., Bölker P., Emberson L., Feng Z., Harmens H., Hayes F., Kobayashi K., Paoletti E., Van Dingenen R. 2018. Ozone pollution will compromise efforts to increase global wheat production. *Glob. Change Biol.* 24: 3560–3574.
- Monks P.S., Archibald A.T., Colette A., Cooper, O., Coyle, M., Derwent D., Fowler D., Granier C., Law K.S., Mills G.E., Stevenson D.S., Tarasova O., Thouret V., von Schneidmesser E., Sommariva R., Wild O. & Williams M.L. 2015. Tropospheric ozone and its precursors from the urban to the global scale from air quality to short-lived climate forcer. *Atmos. Chem. Phys.* 15: 8889–8973.
- Nolte C.G., Spero T.L., Bowden J.H., Mallard M.S. & Dolwich P.D. 2018. The potential effects of climate change on air quality across the conterminous US at 2030 under three Representative Concentration Pathways. *Atmos. Chem. Phys.* 18: 15471–15489.
- Nuvolone D., Petri D. & Voller F. 2018. The effects of ozone on human health. *Environ. Sci. Pollut. Res.* 25: 8074–8088.
- Otero N., Sillman J., Mar K.A., Rust H.W., Solberg S., Andersson C., Engardt M., Bergström R., Bessagnet B., Colette A., Couvidat F., Cuvelier C., Tsyro S., Fagerli H., Schaap M., Manders A., Mircea M., Briganti G., Cappelletti A., Adani M., D'Isodoro M., Pay M.-T., Theobald M., Vivanco M.G., Wind P., Ojha N., Raffort V. & Butler T. 2018. A multi-model comparison of meteorological drivers of surface ozone over Europe. *Atmos. Chem. Phys.* 18: 12269–12288.
- Pellegrini E., Lorenzini G. & Nali C. 2007. The 2003 European heat Wave: Which role for ozone. Some data from Tuscany, Central Italy. *Water Air Soil Pollut.* 181: 401–408.
- Petres S., Lanyi S., Pirianu M., Keresztesi A. & Nechifor A.C. 2018. Evolution of tropospheric ozone and relationships with temperature and NO_x for the 2007–2016 decade in the Ciuc Depression. *Rev. Chim.* 69: 602–608.
- Pio C.A., Feliciano M.S., Vermeulen A.T. & Sousa E.C. 2000. Seasonal variability of ozone dry deposition under southern European climate conditions. *Atmos. Environ.* 34: 195–205.
- Pleijel H., Klingberg J., Pihl Karlsson G., Engardt M. & Karlsson P.E. 2013. Surface Ozone in the Marine Environment — Horizontal ozone concentration gradients in coastal areas. *Water Air Soil Pollut.* 224, 1603, DOI 10.1186/s12940-017-0325-2.
- Russo S., Dosio A., Graversen R.G., Sillman J., Carrao H., Dunbar M.B., Singleton A., Montagna P., Barbola P. & Vogt J.V.M. 2014. Magnitude of extreme heat waves in present climate and their projection in a warming world. *J. Geophys. Res. Atmos.* 119: 12500–12512.
- Sjöqvist E., Abdoush D. & Axen J. 2019. Sommaren 2018 – en glimt av framtiden? SMHI klimatologi Nr 52, 2019. [In Swedish with an English summary] available at https://www.smhi.se/polopoly_fs/1.1491581/Klimatologi_52.pdf
- Solberg S., Hov Ø., Søvde A., Isaksen, I.S.A., Codeville P., De Backer H., Forster C., Orsolini Y. & Uhse K. 2008. *J. Geophys. Res.* 113: D07307.
- Stedman J.R. 2004. The predicted number of air pollution related deaths in the UK during the August 2003 heat-wave. *Atmos. Environ.* 28: 1087–1090.
- Tang L., Chen D., Karlsson P.E., Gu Y. & Ou, T. 2009. Synoptic circulation and its influence on spring and summer surface ozone concentrations in southern Sweden. *Boreal. Env. Res.* 14: 889–902.
- Varotsos K.V., Giannakopoulos C. & Tombrou M. 2019. Ozone-temperature relationships during the 2003 and 2014 heatwaves in Europe. *Reg. Environ. Change* 19: 1653–1665.
- Vieno M., Dore A.J., Stevenson D.S., Doherty R., Heal M.R., Reis S., Hallsworth S., Tarrason L., Wind P., Fowler D., Simpson D. & Sutton M.A. 2010. Modelling surface ozone during the 2003 heat-wave in the UK. *Atmos. Chem. Phys.* 10: 7963–7978.
- World Meteorological Organization (2019). *WMO Statement on the State of the Global Climate in 2018*. WMO-No. 1233, available at https://library.wmo.int/doc_num.php?explnum_id=5789.
- Zhang H., Wang Y., Park T.-W. & Deng Y. 2017. Quantifying the relationship between extreme air pollution events and extreme weather events. *Atmos. Res.* 188: 64–79.